

# Optical transform methods

T.R.Welberry and John M.Thomas

**The diffraction pattern of a crystal or of any known structure may be readily calculated by using fast digital computers. However, it is often scientifically more rewarding, especially for exploring unknown structures or for teaching the subtleties of structural chemistry, to use the simple methods of optical transforms. This article explains why.**

Optical transform methods<sup>1,2</sup> are used predominantly in X-ray crystallography and increasingly in electron microscopy. In X-ray studies the X-ray diffraction pattern from a given material is modelled by using the diffraction of visible light from a suitably scaled pictorial representation of the distribution of atoms and molecules in the original material. In electron microscopy, then high resolution image is used as the 'object' on an optical bench and visible light is diffracted by it to yield a pattern that aids the interpretation of the original micrograph.<sup>3,4</sup>

The idea of using optical analogues to aid in the interpretation of X-ray diffraction patterns originated with Sir Lawrence Bragg around 1938, and the method has developed considerably since then. Before the advent of digital computers the calculation of the diffraction pattern of even a fairly simple crystal structure was an enormous task and so the use of optical diffraction from a model had obvious benefits-particularly for testing trial structures. Once computers were available it became a trivial exercise to calculate the diffraction pattern of an ordered crystal structure for comparison with observed measurements and the optical method began to fall into disuse. On the other hand, for disordered structures, amorphous materials and even liquids the transform method is still used, even though the most complex diffraction patterns can in principle be calculated quite readily with modern computers.

Why should optical transforms remain popular in an age of computer domination? One reason is the method's great power of visual presentation in teaching, in stimulating thought, and in confirming or aiding the development of intuition-which still plays a major role in solving the more complex problems in diffraction. The optical method provides us with an immediate visual check both on the reciprocal space and on real space distributions, and their relative scale and orientation. Moreover, the whole diffraction pattern is obtained immediately and any unexpected features are clearly revealed-features that would perhaps have passed quite undetected in a calculation in which the scale, as well as the required region of the pattern to be calculated and the resolution, must be predetermined.

In recent years methods have been developed to produce routine optical diffraction masks (or screens) for use as aids in interpreting X-ray or electron diffraction patterns.<sup>5,7</sup> We can now produce, rapidly and easily, an optical diffraction mask which is a good representation of almost any real diffraction problem encountered with X-rays or electrons. Although the diffraction patterns obtained may be only qualitatively or at best semiquantitatively in agreement with the real patterns, they provide a useful starting point for interpreting the observations. Examples of problems that we have studied with the aid of such diffraction masks are:

- short range order in molecular crystals;
- size effect distortions in alloys;
- thermal diffuse scattering in minerals;
- small angle scattering in microemulsions;
- fluctuations of local order in liquids.<sup>8-12</sup>

In high resolution electron microscopy, selected regions of the images have been used as the mask,<sup>13</sup> and the resulting diffraction of a laser beam was used to determine the nature of the crystallographic phase-eg 50 $\mu$ m diameter islands of silicon that have crystallized within an annealed thin film of silicon suboxide.

### Diffraction screens and patterns

The screens used in our research are normally produced directly on photographic film by using an Optronics P1700 Photomation film writing device.<sup>5-12</sup> This device can plot points on a basic grid 12.5 $\mu$ m x 12.5 $\mu$ m with an accuracy of ca 1-2 $\mu$ m. On an area of film 10cm x 10cm there are therefore 64 x 10<sup>6</sup> pixels (picture elements) which may be selectively printed. In mask-making, a black dot of one of a small number of possible diameters, eg 50 $\mu$ m, is usually written at selected pixel points. In a typical case ca 5 x 10<sup>5</sup> such dots may be plotted to form the model object.

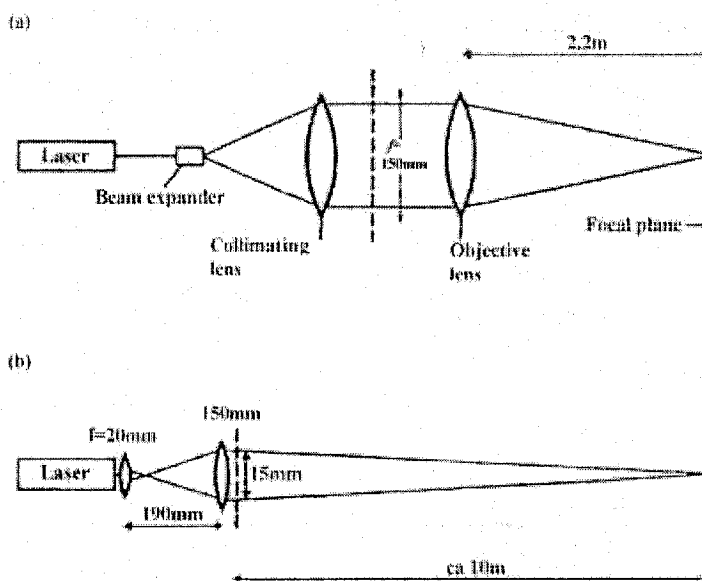


Fig.1. Schematic diagram of the diffractometer used to obtain optical diffraction patterns. (a) The equipment used to obtain high quality patterns with diffraction masks. (b) A simple arrangement suitable for demonstrations in a lecture theatre with smaller diffraction masks of ca 1cm x 1cm, made by photographically reducing those used in (a).

In some cases the computing time required to generate the coordinates to be plotted may be only a few seconds on a VAX computer, while for others many hours may be required. Simple point distributions take only a short time, whereas ones for which long iterative procedures are required-such as Monte Carlo or molecular dynamic simulations-are very slow. The actual plotting time may take up to an hour, depending on the complexity of the mask.

Diffraction patterns are readily obtained by using a laser diffractometer (see Fig.1a). The beam from a small He-Ne laser is passed through a beam expander which consists of a microscope objective, then a small (10 $\mu$ m pinhole) aperture which acts as a spatial filter. The pinhole is at the back focal plane of a collimating lens, L<sub>1</sub>, and is imaged at the focal plane, F of the objective lens, L<sub>2</sub>.

The diffraction pattern of mask M, placed in the parallel portion of the beam, appears at F, where it may be photographed directly by using a camera body without a lens (typically on 35mm or 120 roll film).

If we apply Bragg's law of diffraction,  $\lambda=2d\sin\theta$ , to the optical experiment we find that for a wavelength  $\lambda=0.632\mu\text{m}$  and plotting grid spacing  $d=12.5\mu\text{m}$ , the first order diffraction peaks will occur at a diffraction angle  $\theta=1.448^\circ$ , which corresponds to a distance from the direct beam of 55.6mm in the film plane for our objective lens of 2.2m focal length. We frequently use a scale of one 12.5 $\mu\text{m}$  unit to represent 0.1 $\text{\AA}$  (0.01nm). This means that the region of diffraction space, corresponding to the maximum that can be observed with, say, CuK $\alpha$  X-radiation ( $\sin\theta_{\text{max}}=\lambda/2=0.77\text{\AA}$ ) in a real experiment, falls conveniently within a 35mm frame in the optical analogue experiment.

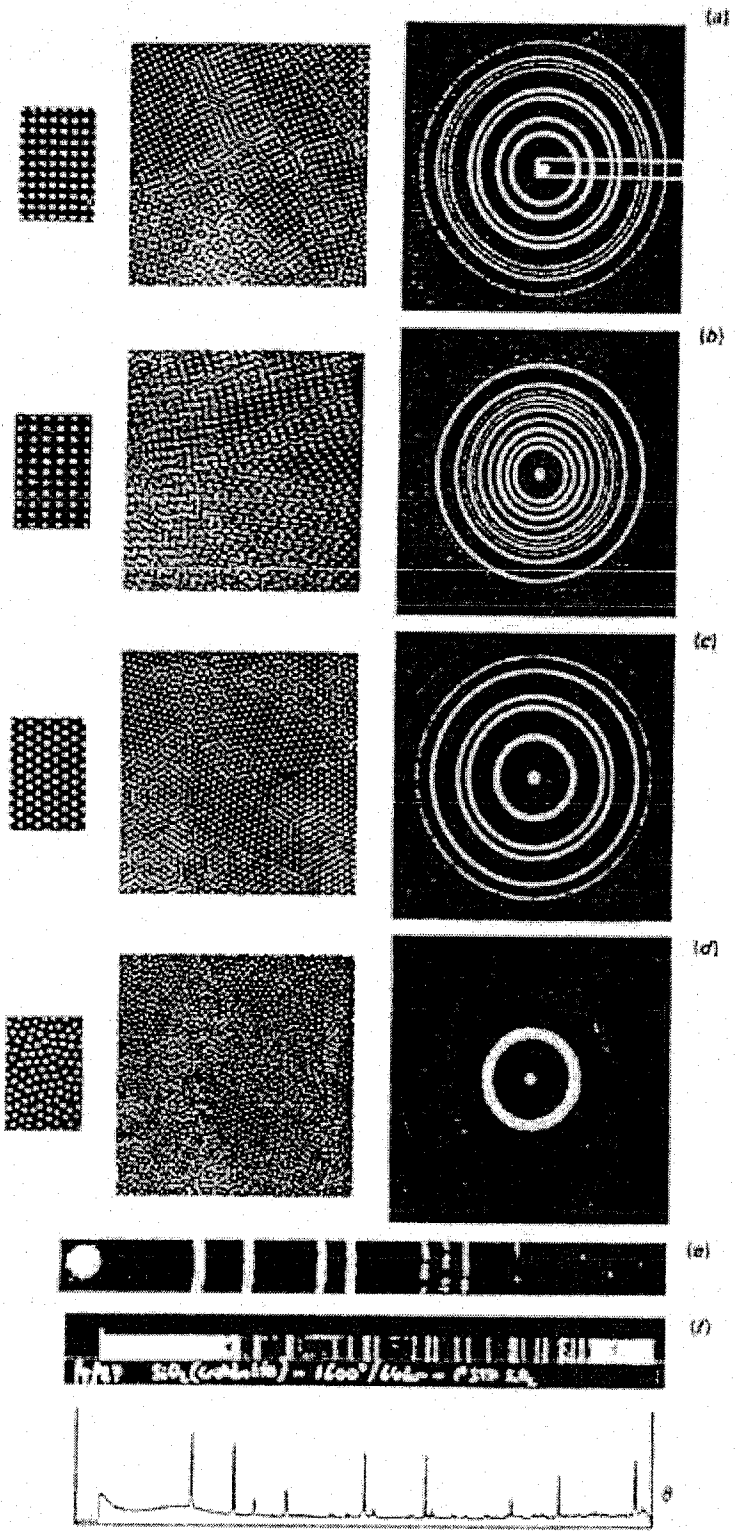


Fig.2. Optical diffraction patterns illustrating the principles of X-ray powder diffraction. (a) Square lattice; (b) rectangular lattice; (c) hexagonal lattice; (d) liquidlike distribution; (e) shows the relation to a real powder photograph-compare with the section shown in (a); (f) shows the diffractogram.

The requirements for demonstration in a lecture theatre are rather different! Here the aim is to produce as large and as large and as visible a diffraction pattern as possible with relatively simple apparatus. The main requirements may be satisfied by reducing the physical size of the diffraction mask by a factor of about 10. Then a laser beam of only about 1cm diameter, easily achieved with small inexpensive lenses, may be

used. With this reduction of scale of the real space representation the diffraction angles are correspondingly larger, and the resulting pattern can be projected onto a distant screen to good effect. *Figure 1b* shows a suitable arrangement. A grid of 20 lines per millimetre gives diffraction peaks with a spacing of about 12cm on a screen at a distance of 10m. For the examples in this article we have used the patterns obtained from the original masks, which were approximately 10cm x 10cm in size, but for the demonstrations these were photographically reduced to about 1cm x 1cm. For some examples, an effective diffraction pattern may be obtained simply by passing the laser beam directly through the reduced mask without any lenses. This is an excellent demonstration for introducing the relationship between the optical and the X-ray experiments, because students find it difficult to see the correspondence if lenses are used in the optical experiment and not in the X-ray experiment.

**Demonstration examples**

There are several useful experiments that can be demonstrated.

1. *X-ray powder patterns.* The aim of this set of examples was to show the type of scattering pattern that is obtained when an X-ray beam is directed onto a polycrystalline sample. Each mask consisted of 441 000 scattering points made up of which contained enough scattering points (a 21 x 21 array) for the diffraction pattern from any one crystallite to display a reasonably good single crystal pattern with sharp Bragg peaks. The individual crystallites were placed at random within the desired area of the mask, and each was given a different orientation. The orientations could have been chosen randomly, but to obtain a reasonably smooth scattered intensity distribution with a relatively small total number of points, they were chosen at equally spaced intervals in the range  $0-\pi$ . Figure 2 shows four different examples. In Fig.2a the lattice is a simple square grid; in Fig.2b it is rectangular with the unit cell edges  $a$  and  $b$  in the ratio 1:1:3; and in Fig.2c it is

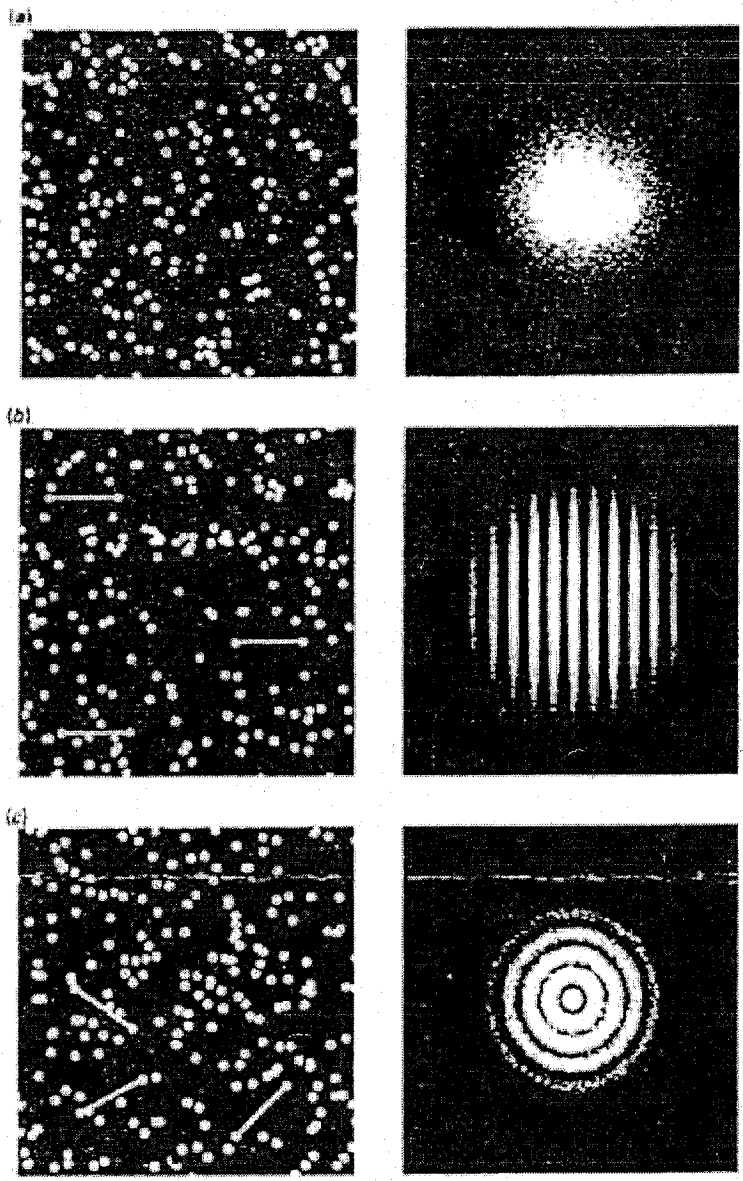


Fig.3. Shows the effectiveness of the optical diffraction pattern in picking out local order not easily seen by the eye in the real space distribution of points. In Fourier space, however-ie in the optical transform-the latent order is apparent:(a)disordered;(b)and(c) have latent order.

hexagonal. On the left we show an enlargement of a small portion of the basic grid on which each example is based, then at a lower magnification we show a small portion of the mask in which a number of crystallites with different orientations can be observed. This is followed by the optical diffraction pattern of the whole mask, showing the complete powder rings of diffraction. We have also expanded a small strip of the pattern for the square lattice (Fig.2e) to emphasize the relationship of the pattern to real X-ray powder photographs. A powder photograph is shown for comparison in Fig.2f together with a diffractogram of the same sample. The pattern for the square grid shows a simple progression of diffraction lines conforming to the simple rule:

$$\frac{\sin\theta}{\lambda} = \frac{(h^2+k^2)^{1/2}}{2a}$$

where h and k are integers and a is the length of the unit cell edge. Note that  $(h^2+k^2)$  may take values 1,2,4,5,8,9,10,13,16,17,18,20 etc. The gaps in the progression where 3,6 and 7,11 and 12, and 14 and 15 should be, are clearly visible. A much more complex powder pattern containing more diffraction lines is obtained for the rectangular lattice, for which the corresponding formula is,

$$\frac{\sin\theta}{\lambda} = 1/2 \left( \frac{h^2}{a^2} + \frac{k^2}{b^2} \right)^{1/2}$$

while for the hexagonal lattice fewer diffraction lines appear, at values of the diffraction angle given by,

$$\frac{\sin\theta}{\lambda} = \frac{(h^2+hk+k^2)^{1/2}}{\sqrt{3}a}$$

To demonstrate the difference between these polycrystalline solids and an amorphous material we also constructed a diffraction mask with a liquid-like structure (Fig.2d). Although the average nearest neighbour distance is the same as for the hexagonal lattice of Fig.2c, the range of order is very short. Each small region of the mask was in fact plotted from the coordinates obtained from a molecular dynamic simulation of a simple liquid—a necessarily large computation even with a relatively small number of atoms. The same set of coordinates was used many times with different orientations to produce a mask containing a sufficiently large total number of particles. The diffuse rings in the diffraction pattern of this example occur in positions corresponding to the first three powder rings in Fig.2c.

2. Local order and disorder. Observation of the local order and the more macroscopic disorder apparent in the examples of Fig.2 leads naturally onto a discussion of what exactly is meant by disorder, and Fig.3 illustrates that the visual appearance of a distribution of points can be misleading. Each of the three examples shown in Fig.3 appears to be simply a disordered collection of points. The sections illustrated are small representative regions of the masks used to obtain the optical diffraction patterns, each mask again containing ca 400 000 points. Of the three distributions, however, only that in Fig.3a is totally random. By random we mean that each point is placed on the area of the diffraction mask quite independently of all other points. In Fig.3b the points are all in pairs, so that for every point that is visible a second point may be found at a fixed distance away in the horizontal direction. Some sample pairs of points have been identified by drawing the connecting line - this is not easily detected by eye because for any point the several closest neighbours do not include the one to which it is paired. The pairing is, however, very apparent in the diffraction pattern. The spacing of the fringes is inversely proportional to the length of the pairing vector. In Fig.3c similar pairs of points have been placed randomly but now the orientation of the connecting vector is also chosen randomly. The pairs, some examples of which are shown, are now more difficult to distinguish even on close scrutiny, but their presence is clearly evident in the diffraction pattern.

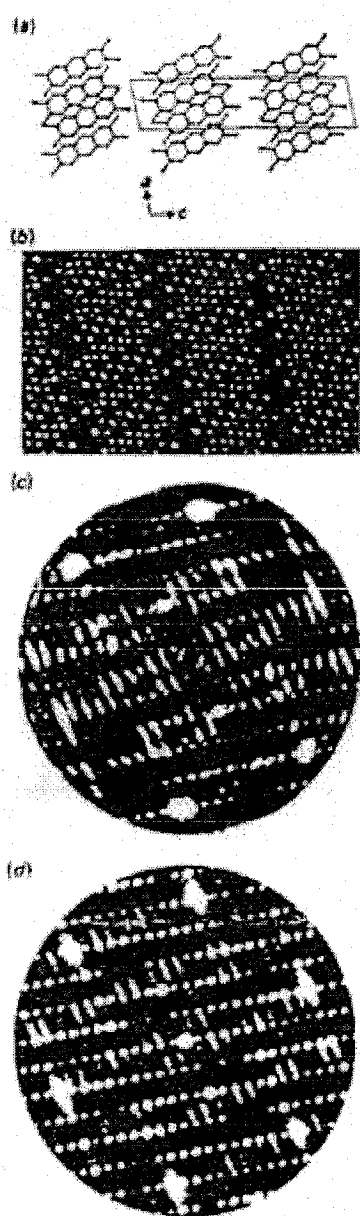


Fig.4. Example of a disordered molecular crystal, 2,3-dichloro-6,7-dimethylantracene: (a) - a drawing of the crystal structure assuming that all molecules are in an ordered arrangement; large circles represent chlorine atoms and small circles carbon; (b) a small portion of a diffraction mask representing the disordered structure in which some molecules are rotated by  $180^\circ$ ; (c) the real X-ray diffraction pattern; (d) the optical diffraction pattern obtained from a model which included both the static disorder and thermal displacements.

3. Disorder in molecular crystals. Molecular crystals provide a wide range of examples of interesting and instructive X-ray diffuse scattering, which can be modelled well by the optical method. There are numerous instances in which a type of static disorder occurs because the molecule can fit into the crystal in one of two different orientations without disturbing the overall repetitive pattern. Figure 4 shows an example of such a crystal - 2,3-dichloro-6,7-dimethylantracene.<sup>5</sup> Figure 4a shows a drawing of the average crystal structure and it is clear that in each molecular site a molecule can be rotated by  $180^\circ$ , effectively interchanging the methyl and chloro substituents, with very little apparent change in the shape presented to the surrounding molecules. For this example there is so little difference in energy between the two different orientations that these disorientations occur very frequently in a crystal. Such mistakes can clearly be seen in the small portion of a typical diffraction mask, which is shown in Fig.4b (the complete mask contained ca 300 000 dots). In the mask the larger dots represent the chlorine positions and the smaller dots the carbon. The resulting disorder gives rise to strong diffuse diffracted intensity called disorder diffuse scattering (DDS). In addition, further thermal diffuse scattering (TDS) occurs as a result of the thermal

motion of the molecules. The optical diffraction pattern shown in Fig.4d includes both of these effects and can be seen qualitatively to be in good agreement with the observed X-ray pattern (Fig.4c). The DDS is observed as sets of diffuse bands connecting the rows of sharp Bragg peaks, while the TDS is seen as rather broader regions of scattering most evident in six stronger peaks near the periphery of the pattern. The DDS bands of intensity occur normal to the directions in the crystal in which short range order exists. The orientation of any one molecule is not completely random, but is strongly influenced by the orientation of neighbouring molecules, particularly those making end-to-end contact. The model also reproduces fairly well the variation of the Bragg peak intensities.

4. Quasicrystals - fivefold symmetry. There has been much interest recently in the topic of so-called quasicrystals.<sup>14</sup> Quasiperiodic crystals (to give them their full name) are a new class of aperiodic atomic structures which have noncrystallographic point symmetries, but which nevertheless give diffraction patterns with sharp diffraction peaks indicative of long range order. A number of binary metallic alloy as well as other systems form phases displaying such quasiperiodic properties.<sup>15</sup> A convenient two dimensional example, suitable for demonstration, is simple Penrose tiling (Fig.5a).<sup>16,17</sup> In contrast to the conventional concept of a crystal structure, in which the same basic unit is repeated by translational symmetry to produce a perfectly periodic array, here two different tiles—the so-called thin and fat rhombs—are packed together in a perfectly prescribed but aperiodic pattern. To generate the Penrose tiling pattern an iterative procedure is used which does and hierarchical subdivision of each rhomb. In Fig.5a the heavy lines represent one stage of the subdivision process for a small section of tiling. Each fat and thin rhomb is then subdivided as indicated by the lighter lines to form the next generation of the subdivision. Once the tiling pattern has been generated it may be decorated by positioning scattering points in a variety of ways on each of the different rhombs in the same way as a crystal structure is formed from a lattice of points. At present, very little is known of the actual atomic arrangements in real quasicrystals. Accordingly we show an example in which scattering points are placed at the corners of each rhomb. A small portion of the diffraction mask, which contained a total of ca  $10^8$  scattering points, is shown in Fig.5b, and the optical diffraction pattern is shown in Fig.5c. It should be noted that although the tiling pattern has fivefold symmetry, the diffraction pattern has tenfold symmetry because the diffraction process always adds inversion symmetry to the real space symmetry.

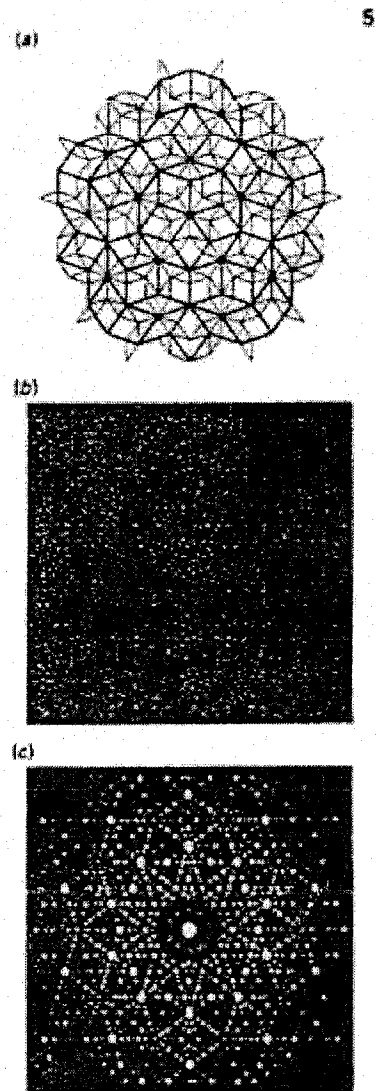


Fig.5.(a) The Penrose tiling pattern showing the fat and thin rhombs, and the fivefold symmetry. (b) A small region of the diffraction mask. (c) The optical diffraction pattern.

5. Diffraction from helices. As a final example we show the diffraction patterns of some simple helices, which illustrate the characteristic patterns of many



macromolecules, eg helical polysaccharides (collagen), complex linear (gellan) and branched (xanthan) polysaccharides, nucleic acids, fibrous macromolecular assemblies (bobby virus, bacteriophages etc)-and some membrane structures that form two dimensional periodic arrays.<sup>18</sup> Because these molecules do not form extensive regular crystals they are not generally amenable to conventional crystallographic analysis. Nevertheless, diffraction has played an important role in determining the structures of DNA and of a wide range of other linear bipolymers, because specimens can be prepared in which the long axes of the molecules are approximately parallel. The molecules sometimes further organize laterally into small regions of three dimensional crystallinity, although the orientations of the crystallites about their long axes are random.

In the examples shown in Fig.6 each diffraction mask consisted of 500 helical chains placed randomly within the frame of the mask. Each chain contained ca 900 scattering points and each had the same orientation, but, because the centres of mass were quite arbitrary, there was no correlation between the phases of the helix in neighbouring chains. Only two examples are given; they show the effect of altering the pitch of the helix. Many other variations of the mask could be generated to show such effects as varying the chain orientation, varying the degree of alignment of neighbouring chains, including a second helix to form a double helix etc. In

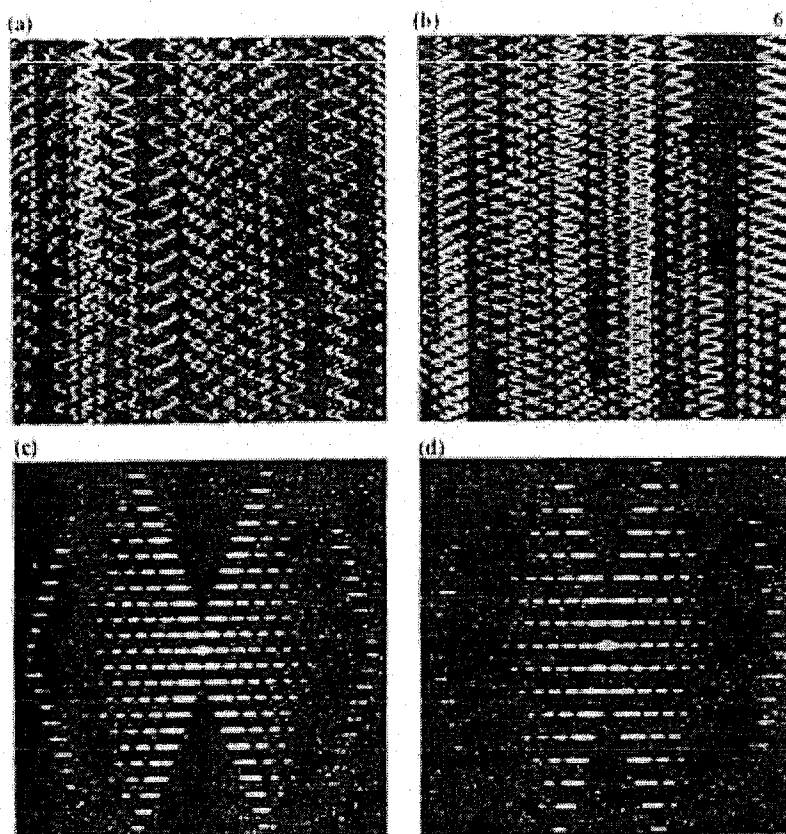


Fig.6(a) and (b) Diffraction masks; (c) and (d) the corresponding diffraction patterns. The only difference between (a) and (b) is the pitch of the helix.

each of the examples shown the X-shaped pattern of diffraction peaks characteristic of a helical structure is easily discerned. There is also a resemblance of the horizontal rows of peaks to an ordinary X-ray rotation photograph of a single crystal.

To drive home the message that an X-shaped diffraction pattern implies a helical structure in real space, one need only place the coiled coil (helical) filament from a domestic electric light bulb in the path of a weak Ke-Ne laser beam, such as that used in a modern red laser pointer. The similarity between the resulting optical diffraction and the X-ray pattern first recorded<sup>19</sup> by Rosalind Franklin for DNA is striking.



Optical transforms are currently used in a wide variety of structural contexts, as a glance at the primary journals devoted to condensed matter and surfaces will reveal. Apart from the illustrations given in this article, you may be interested to hear how useful they have been in determining whether metallic organosols are crystalline,<sup>20</sup> or whether two dimensional adsorbed layers are ordered.<sup>21</sup> Optical transforms are however, of great pedagogic value, and may be used to introduce the concepts of packing and structure, and the architecture of crystals to a young audience unacquainted with X-ray phenomena.

Dr Richard Welberry is senior fellow in the research school of chemistry, Australian National University, GPO Box 4, Canberra City, ACT 2601, Australia; John M. Thomas is Fullerian professor and director at the Davy-Faraday Research Laboratory, The Royal Institution, 21 Albemarle Street, London W1X4BS.

---

Many of the illustrations shown here were prepared for the Royal Institution Christmas Lectures 1987, given by J.M.T.

---

#### References

1. H.S.Lipson, *Optical transforms*. New York: Academic, 1973.
2. G.Harburn, C.A.Taylor and T.R.Welberry, *An atlas of optical transforms*. London: Bell, 1975.
3. G.R.Millward and J.M.Thomas, proceedings of the *Carbon and graphite conference*, p 492. London: Society of Chemical Industry, 1974.
4. J.M.Thomas *et al.*, *J. Chem. Soc., Faraday Trans.2*, 1983, 79, 1075.
5. T.R.Welberry and R.D.G.Jones, *J.Appl. Crystallogr.*, 1980, 13, 244.
6. T.R.Welberry and C.E.Carroll, *Acta Crystallogr.*, 1982, A38, 761.
7. T.R.Welberry and R.L.Withers, *J.Appl. Crystallogr.*, 1987, 20,280.
8. T.R.Welberry, R.D.G. Jones and J.Epstein, *Acta Crystallogr.*, 1982, B38, 1518.
9. T.R.Welberry, *J.Appl. Crystallogr.*, 1986, 19, 382.
10. G.L.Hua, T.R.Welberry and R.L.Withers, *J.Phys. C*, 1988, 21, 3863.
11. T.R.Welberry and T.N.Zemb, *J.Colloid Interface Sci.*, 1988, 123, 413.
12. H.J.M.Hanley *et al.*, *Phys. Rev. A.*, 1988, A38, 1628.
13. J.Wong *et al.*, *J.Chem. Soc., Chem. Commun.*, 1986, 359.
14. D.Shechtman *et al.* *Phys. Rev. Lett.*, 1985, 53, 1951.
15. N.Thangaraj *et al.*, *J.Microsc.*, 1987, 146, 287.
16. M.Gardner, *Sci. Am.*, 1977, 236, 110.
17. N.G de Bruijn, *Mathematics*. 1981, A84, 39.
18. R.P.Millane, *Computing in crystallography 4*, N.W.Isaacs and M.R.Taylor (eds). Oxford: OUP, 1988.
19. R.E.Franklin and R.Gosling. *Nature (London)*, 1953, 171, 740.
20. A.C.Curtis *et al.* *Angew. Chem., Int. Ed. Engl.*, 1988, 27, 1530.
21. M.W.Roberts and C.S.McKee, *Chemistry of the metal-gas interface*. Oxford OUP, 1978.

